

# **Nonlinear Diffusion in Magnetized Discharges**

Francis F. Chen

Electrical Engineering Department

PPG-1579

January, 1998  
Revised April, 1998

# Nonlinear Diffusion in Magnetized Discharges

Francis F. Chen

*Electrical Engineering Department, University of California, Los Angeles, California 90095-1594*

## ABSTRACT

In high-density gas discharges in which the electrons, but not the ions, are confined by a magnetic field, the radial density profile is often observed to have a triangular shape, as if the ionization were concentrated on axis. However, such profiles can also result from nonlinear diffusion, in which the diffusion coefficient varies inversely with density.

## I. INTRODUCTION

Magnetically enhanced inductive discharges are often used to produce high density plasmas for industrial purposes. Research on helicon discharges in uniform cylinders, for instance, is being pursued in many laboratories in order to study the behavior of partially ionized plasmas with a DC magnetic field capable of confining the electrons but not strong enough to confine the ions. In such discharges, the radial density profile is sometimes observed to have a triangular shape [1]. A recent example of such a profile is shown in Fig. 1 [2]. If radial diffusion is controlled by diffusion in a background of neutrals, one would expect a convex density profile; for instance, a  $J_0$  Bessel function if the ionization is proportional to electron density [3]. A concave or straight profile would suggest that ionization is heavily concentrated on axis, in contradiction to theoretical results on the coupling of helicon waves to Trivelpiece-Gould modes near the surface [4]. In this paper we explore the possibility that these strange profiles are caused by an unusual classical diffusion mechanism.

## II. DIFFUSION IN INTERMEDIATE MAGNETIC FIELDS

Consider an infinitely long plasma column confined in a tube of radius  $a$  with a coaxial DC magnetic field  $\mathbf{B}_0$  of 50-1500 G magnitude. In this field, electrons will usually have Larmor radii  $r_L$  much smaller than  $a$ , but heavy ions, such as argon, will have  $r_L \gg a$ . Ions will diffuse radially outward, impeded by collisions with the neutral gas; but they will also be impeded by collisions with electrons, since the electrons are restrained by the magnetic field and cannot easily move radially with the ions. The physical picture is that the slowly drifting ions are continuously bombarded by electrons moving along  $B_0 \hat{z}$ . The momentum exchange is mostly in the  $z$  direction, but the small amount of *radial* momentum that the ions lose to the electron "rods" is what impedes ion loss. In principle, there should be an ambipolar electric field slowing the radial ion motion, but in practice such fields are not usually observed. Radial variations in potential tend to be weak and of the wrong sign to give an ambipolar field [5]. Fig. 2 shows a radial profile of plasma potential obtained from the inflection point of the  $I$ - $V$  characteristic of a fully RF-compensated Langmuir probe [2]. The plasma potential does not follow the density variation, and the radial E-field is too weak to affect the ion motions.

The absence of an inward pointing E-field is expected only if axial transport can be neglected, as in very long discharges. In the opposite limit of isotropic diffusion, one would expect the electrons to thermalize into a Boltzmann distribution  $n_e = n_0 \exp(eV/KT_e)$ , so that the potential follows the density profile and the E-field points outwards. In the intermediate case of magnetized discharges of finite length, the short-circuit effect comes into play. In this

mechanism, the sheath drop on the end wall terminating each magnetic field line can adjust itself to bleed off excess electrons on that field line (or to cure a deficit of electrons by erecting a higher Coulomb barrier) so as to maintain a self-consistent radial E-field. Though a detailed calculation is almost impossible because electron motions can also be affected by high-frequency instabilities, the result can be the near-elimination of the radial E-field, as is observed. We therefore neglect the radial electric field from now on and consider the diffusion of ions in a background of neutrals and “stiff” electrons.

The total ion collision frequency is given by

$$\mathbf{n} = \mathbf{n}_{ie} + \mathbf{n}_{in} + \mathbf{n}_{ii}, \quad (1)$$

where the last term represents ion-ion collisions, which can safely be neglected since there is no shear flow. The singly ionized ion-electron collision frequency  $\mathbf{n}_{ie}$  is given by Book [6] as

$$\mathbf{n}_{ie} = 1.6 \times 10^{-9} n_e \ln \Lambda / A_i T_e^{1/2} E_i, \quad (2)$$

where  $A_i$  is the ion mass number,  $T_e$  is the electron temperature in eV,  $E_i$  is the ion energy, and the Coulomb logarithm  $\ln \Lambda$  for these plasma is about 10.7. For a Maxwellian ion distribution, we may approximate  $E_i$  by  $(3/2)T_i$ .

The ion-neutral collision frequency  $\mathbf{n}_{in}$  is dominated by charge exchange, the cross section for which is given for low energies by Sheldon [7]. Since this was found to agree with mobility data, we can also infer  $\mathbf{n}_{in}$  from the measured mobility of  $\text{Ar}^+$  in Ar, namely,  $1.5 \text{ cm}^2/\text{V}\text{-sec}$  at 760 Torr and 296°K [8]. This yields

$$\mathbf{n}_{in} = 2.05 \times 10^4 p_o (\text{mTorr}). \quad (3)$$

The critical density above which ion-electron collisions are dominant over ion-neutral collisions is therefore given by

$$n_{crit} = 2.05 \times 10^4 \frac{p_o}{\mathbf{n}_{ie} / n_e}. \quad (4)$$

For  $T_e = 3 \text{ eV}$  and  $T_i = 0.0257 \text{ eV}$  in argon, this gives  $n_{crit} \approx 10^{13} \text{ cm}^{-3}$ , a rather high value even with room temperature ions. However, at these densities the neutral pressure inside the plasma is reduced by the ion-pumping effect, which was inferred by Sudit and Chen [5] and has since been confirmed by direct measurement [9].

To estimate the ion pumping effect, consider a plasma of radius  $a$  and length  $L$ , so that the volume  $V$  is  $V = \pi a^2 L$ . Initially, gas is bled in at a flux  $\mathbf{G}_{in}$  atoms/sec and pumped out at a rate  $S \text{ cm}^3/\text{sec}$ , resulting in a fill pressure  $p_o$  (mTorr) and a neutral density  $n_{n0} = p_o N_0$ , where  $N_0 = 3.3 \times 10^{13} \text{ cm}^{-3}$  at 300°K. After the discharge is struck, the neutrals inside the plasma are ionized, and ions with an average density  $n_i$  are accelerated by the pre-sheath electric field toward the pump at one end of the discharge tube. We assume that the pump manifold is large enough to remove the recombining ions without appreciable refluxing of the neutrals, and we neglect the transit time of the accelerated ions. Next, we compute the neutral density  $n_{n1}$  in the chamber when the plasma is on. The flux of atoms leaving the plasma at both ends is  $dN_i/dt = -2\pi a^2 \cdot 1/2 n_i c_s$ , where  $c_s$  is the ion sound speed  $(KT_e/M)^{1/2}$  and  $1/2 n_i$  is the ion density at the sheath edge. Ions are created at the rate  $dN_i/dt = \pi a^2 L n_e n_{n1} P_i$  where  $P_i \equiv \langle \sigma v \rangle_{ion}$  is the ionization probability, a sensitive function of  $T_e$ . Equating this to the loss rate, we find that  $n_e = n_i = n$  cancels, and  $n_{n1}$  is given by

$$n_{n1} = c_s / LP_i . \quad (5)$$

If  $G_{in}$  is not measured, we can find  $n_{n0}$  as follows. Neutrals are lost at the rate that ions are lost at the pump end of the tube:

$$G_{out} = pa^{2/2}n_i c_s . \quad (6)$$

Equating this to  $G_{in} = Sn_{n0}$ , we have

$$n_{n0} = pa^{2/2}n_i c_s / S . \quad (7)$$

The pressure reduction ratio is therefore given by Eqs. (5) and (7) as

$$e \equiv \frac{n_{n1}}{n_{n0}} = \frac{2S}{Vn_e P_i} . \quad (8)$$

Since the diffusion coefficient for unmagnetized particles is given by  $D = KT/Mv$ , Eq. (2) leads to

$$D_{ie} = 8.4 \times 10^{19} T_e^{1/2} T_i^2 / n_e , \quad (9)$$

while Eq. (3) gives (for argon)

$$D_{in} = 1.2 \times 10^6 T_i / p_0 . \quad (10)$$

Substituting  $\epsilon p_0$  for  $p_0$  in Eq. (10) and solving for  $n_e$ , we obtain

$$n_{crit} = (1.4 \times 10^{17} T_e^{1/2} T_i S / VP_i)^{1/2} . \quad (11)$$

For instance, for  $T_e = 3$  eV,  $T_i = 0.1$  eV (assuming some heating by the electrons),  $S = 10^5$  cm<sup>3</sup>/sec, and  $a = 5$  cm,  $n_{crit}$  is  $1.2 \times 10^{12}$  cm<sup>-3</sup>. As  $T_e$  ranges from 2 to 5 eV,  $n_{crit}$  changes from  $5 \times 10^{12}$  to  $4 \times 10^{11}$  cm<sup>-3</sup>, densities usually well exceeded in the experiments in question. We may therefore neglect diffusion via ion-neutral collisions.

### III. RADIAL PROFILES

In the previous section we have tried to justify the neglect of  $n_{in}$ ; we now explore the consequences if this approximation is reasonable. With the use of Eq. (2) the ion diffusion coefficient is given by

$$D = \frac{KT_i}{Mn_{ie}} \equiv \frac{A}{n} , \quad (12)$$

where the constant  $A$  is of order  $10^{17}$  cm<sup>-1</sup>sec<sup>-1</sup> (argon,  $T_i = 0.0257$  eV,  $T_e = 3$  eV). Thus,  $D$  varies as  $1/n$ , rather than as  $n$ , as for perpendicular diffusion of a fully ionized and fully magnetized plasma [3]. The steady-state equation of continuity is

$$\nabla \cdot (D\nabla n) + Q = 0 . \quad (13)$$

Neglecting longitudinal **ion** diffusion in a long, thin cylinder, we have

$$\frac{A}{r} \frac{d}{dr} \left( \frac{r}{n} \frac{dn}{dr} \right) + Q = 0 . \quad (14)$$

### 1. Case of $Q = \text{constant}$

If the source term is uniform, the finite solution of Eq. (9) is

$$\ln n = C - \frac{Q}{4A} r^2. \quad (15)$$

If we apply the boundary conditions  $n = n_0$  at  $r = 0$ ,  $n = \delta n_0$  at  $r = a$ , the density profile depends only on the edge density and is given by

$$\frac{n}{n_0} = \mathbf{d}^{r^2/a^2}. \quad (16)$$

Fig. 3 shows such profiles for several values of  $\delta$ . Though these Gaussians are closer to Fig. 1 than Bessel functions, they are still not sufficiently “triangular.” Uniform ionization can apply, for instance to discharges ionized by ultraviolet light or fast electron beams, such as in E-beam excited CO<sub>2</sub> lasers.

### 2. Case of $Q$ proportional to $n$

The ionization frequency per unit volume is given by

$$Q = n_n n_e \langle \sigma v \rangle_{\text{ion}} \equiv G n_e, \quad (17)$$

where the ionization probability  $\langle \sigma v \rangle_{\text{ion}}$  is sensitive to  $T_e$ . Eq. (9) now becomes

$$\frac{d}{dr} \left( \frac{r}{n} \frac{dn}{dr} \right) = - \frac{G}{A} n r. \quad (18)$$

Changing to dimensionless variables  $n^* = n/n_0$ ,  $r^* = r/a$ , and  $(\prime) = a(d/dr)$ ; defining

$$q \equiv G n_0 a^2 / A; \quad (19)$$

and then dropping the (\*), we obtain

$$n'' + \left( \frac{1}{r} - \frac{n'}{n} \right) n' + q n^2 = 0. \quad (20)$$

Values of  $q$  for various temperatures and densities are shown in Fig. 4, and numerical solutions of Eq. (20) for various values of  $q$  are shown in Fig. 5. These density profiles are “triangular” only for intermediate values of  $q$ . The curve for  $q = 10$  resembles not only Fig. 1 but also profiles measured by L. Porte [10] in an entirely different machine: 2.5-cm radius, 20 mTorr, and 800G, with  $T_e = 3$  eV and peak density  $\approx 3 \times 10^{13}$  cm<sup>-3</sup>, parameters for which  $q = 10$  is appropriate.

### 3. Case of bimodal energy deposition

Numerical computations of energy deposition by coupled helicon and Trivelpiece-Gould (TG) waves [4] usually show two peaks, one near the surface due to TG absorption, and one near the axis due to helicon absorption. An example of such a bimodal energy deposition profile is shown in Fig. 6, calculated for a high-field discharge<sup>11</sup>. Local deposition of RF energy raises  $T_e$  locally and increases  $\langle \sigma v \rangle_{\text{ion}}$ , and hence  $q$  there. We have modeled this situation by using a function  $q(r)$  consisting of two Gaussians centered at different radii. An ex-

ample is shown in Fig. 7, where it is seen that the resulting profile  $n(r)$  is “triangular,” resembling the measured data shown in Fig. 1 and reproduced in Fig. 7.

#### **IV. Summary**

Transverse diffusion of fully ionized plasmas in intermediate magnetic fields is shown to be governed by a diffusion coefficient inversely proportional to the density. The assumption of complete ionization is valid over a density range applicable to high-density plasma sources if the ion pumping effect is taken into account. This nonlinear diffusion, coupled with a physically reasonable RF absorption profile, can lead to the triangular density profiles observed experimentally in helicon discharges.

## REFERENCES

1. G. Chevalier and F.F. Chen, *J. Vac. Sci. Technol. A* **11**, 1165 (1993).
2. D.D. Blackwell, Master's Thesis, UCLA (1994). The data shown were taken more recently in the same machine.
3. F.F. Chen, *Introduction to Plasma Physics and Controlled Fusion*, 2nd ed., Vol. 1, Chap 5 (Plenum Press, New York).
4. D. Arnush and F.F. Chen, *Phys. Plasmas* **5**, xxxx (1998).
5. I.D. Sudit and F.F. Chen, *Plasma Sources Sci. Technol.* **5**, 43 (1996), Fig. 10.
6. D.L. Book, *NRL Plasma Formulary*, Publication 0084-4040, Naval Research Laboratory, Washington, DC 20375-5320.
7. J.W. Sheldon, *Phys. Rev. Lett.* **8**, 64 (1962).
8. E.W. McDaniel and E.A. Mason, *Mobility and Diffusion of Ions in Gases* (Wiley, New York, 1973), p. 274.
9. J. Gilland and N. Hershkowitz, *Bull. Amer. Phys. Soc.* **42**, 1751 (1997).
10. L. Porte, *Bull. Amer. Phys. Soc.* **42**, 1818 (1997).
11. D. Arnush and F.F. Chen, UCLA Report PPG-1573 (1997).

## FIGURE CAPTIONS

1. Typical "triangular" density profile, with  $a = 5$  cm,  $B_0 = 640$ G,  $p_0 = 3$  mTorr of argon,  $P_{rf} = 1$  kW at 13.56 MHz [2].
2. Radial profiles of density, space potential  $V_s$ , and floating potential  $V_f$  for a 10-cm diam discharge at 600 G, 6 mTorr, and 1.5 kW at 13.56 MHz [2].
3. Computed density profiles for uniform ionization.
4. Dependence of the dimensionless parameter  $q$  on density and temperature, for  $T_i = 0.05$  eV,  $p_0 = 3$  mTorr,  $a = 5$  cm.
5. Computed density profiles for ionization proportional to density. The curves are in the same order as in the legend.
6. Plasma loading as a function of radius, computed for a half-wavelength  $m = +1$  helical antenna and a triangular density profile. Other parameters were:  $B_0 = 1$  kG,  $n = 10^{13}$  cm<sup>-3</sup>,  $p_0 = 3$  mTorr of argon, and  $f = 27.12$  MHz [11].
7. Density profile computed for a spatially varying source of plasma heating, as shown by the broad line. The points are the data of Fig. 1.

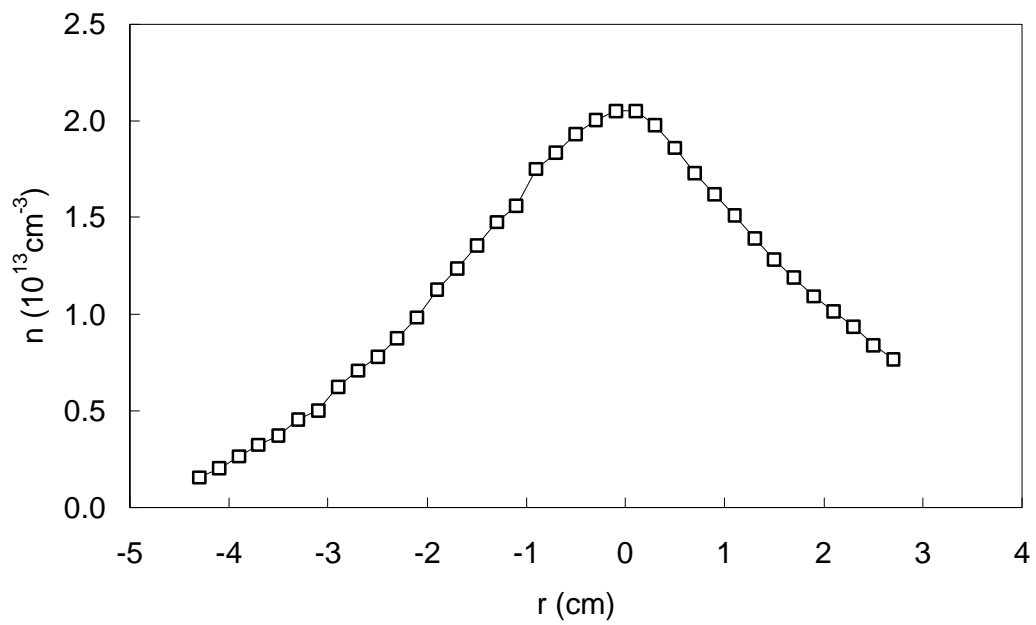


Fig. 1

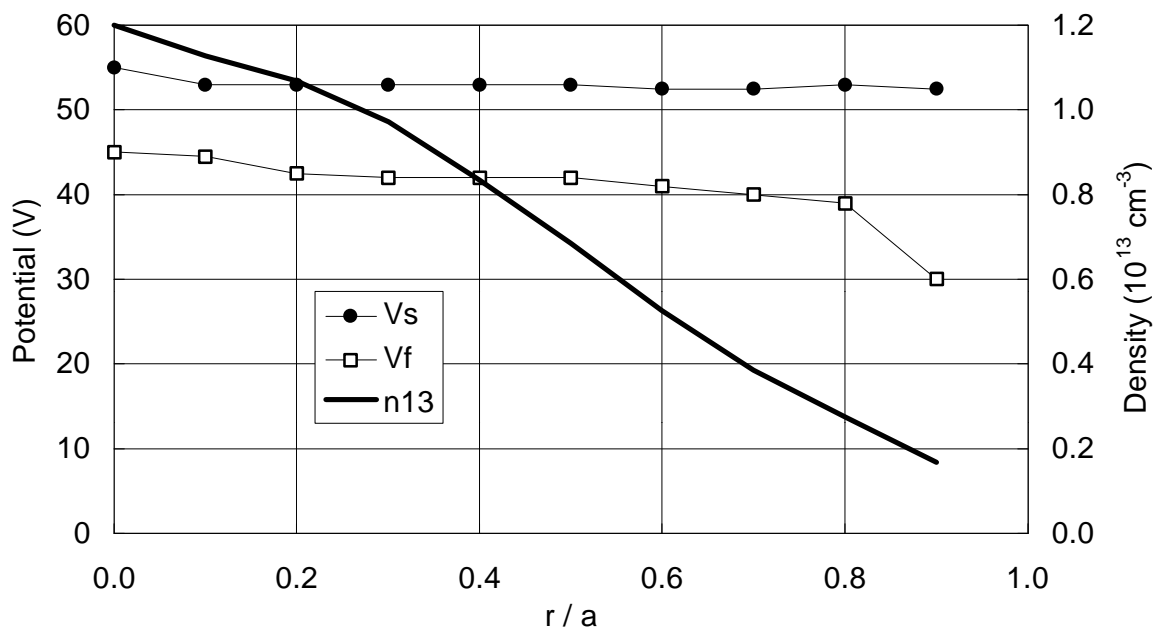


Fig. 2

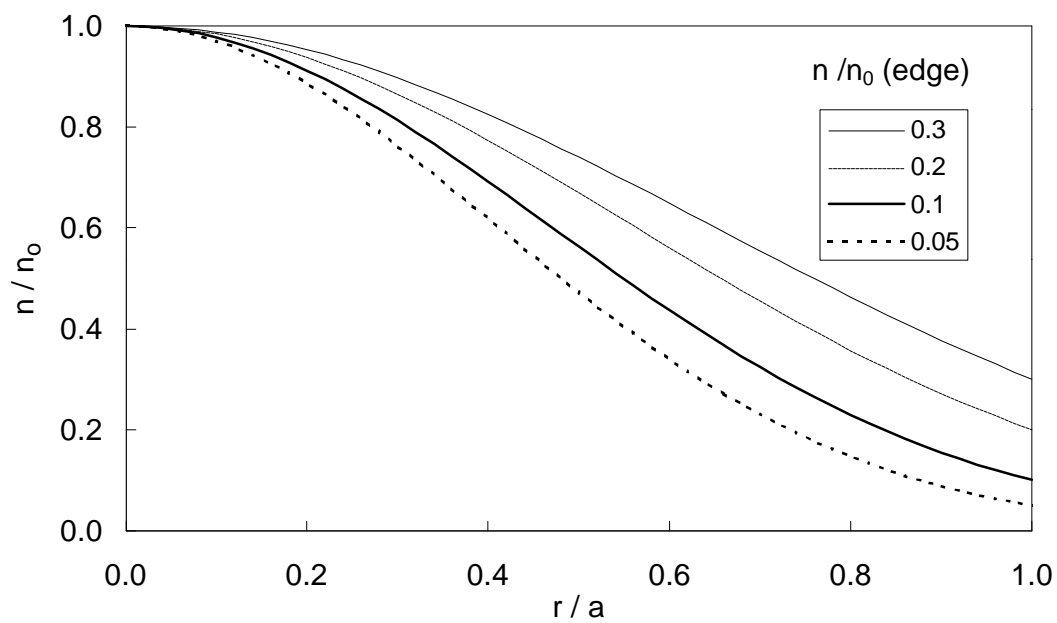


Fig. 3

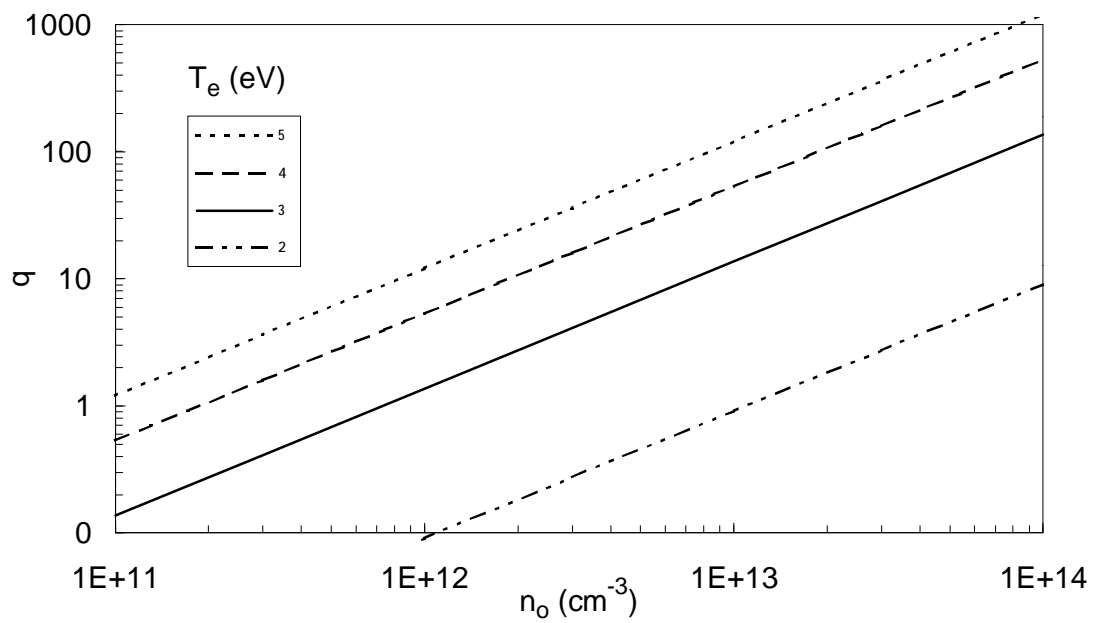


Fig. 4

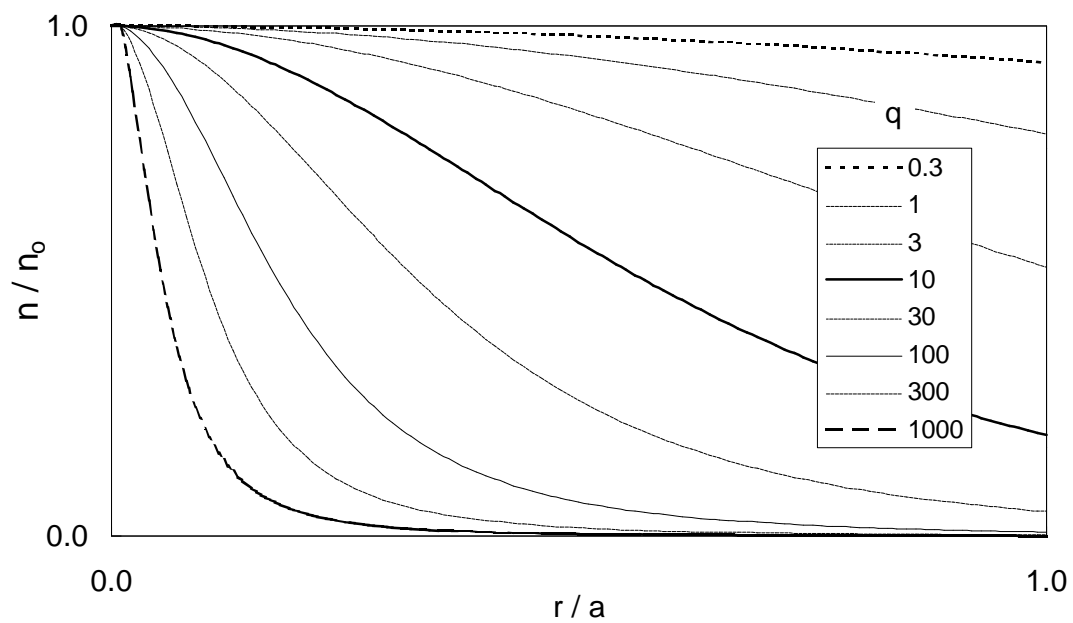


Fig. 5

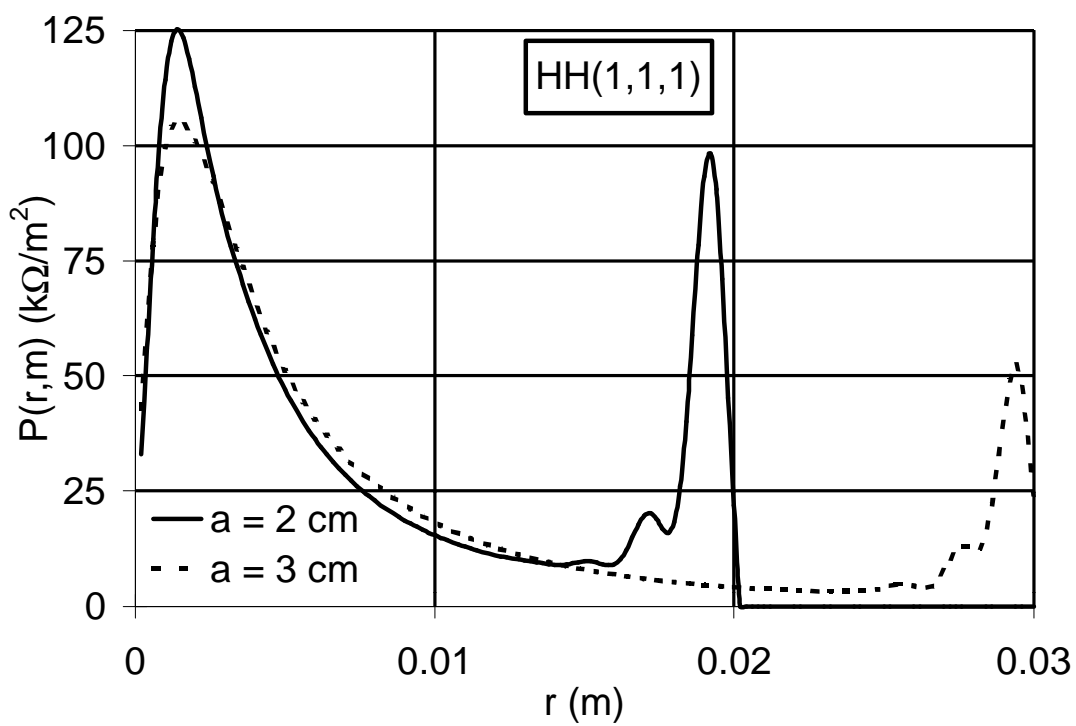


Fig. 6

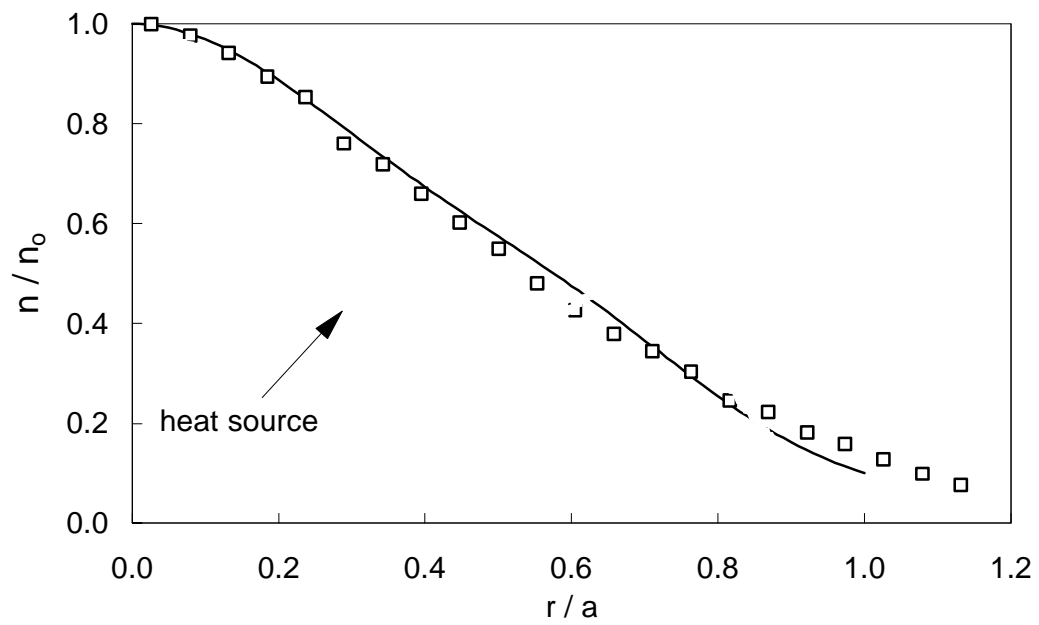


Fig. 7